

This discussion paper is/has been under review for the journal Biogeosciences (BG).
Please refer to the corresponding final paper in BG if available.

Distributions and stoichiometry of dissolved nitrogen and phosphorus in the iron fertilized region near Kerguelen (Southern Ocean)

S. Blain^{1,2}, J. Capparos^{1,2}, A. Guéneuguès^{1,2}, I. Obernosterer^{1,2}, and L. Oriol^{1,2}

¹Sorbonne Universités, UPMC Univ Paris 06, UMR7621, Laboratoire d’Océanographie Microbienne, Observatoire Océanologique, 66650 Banyuls/mer, France

²CNRS, UMR7621, Laboratoire d’Océanographie Microbienne, Observatoire Océanologique, 66650 Banyuls/mer, France

Received: 13 June 2014 – Accepted: 17 June 2014 – Published: 27 June 2014

Correspondence to: S. Blain (stephane.blain@obs-banyuls.fr)

Published by Copernicus Publications on behalf of the European Geosciences Union.

BGD

11, 9949–9977, 2014

Distributions and stoichiometry of dissolved nutrients in the Southern Ocean

S. Blain et al.

Title Page

Abstract

Introduction

Conclusions

References

Tables

Figures

◀

▶

◀

▶

Back

Close

Full Screen / Esc

Printer-friendly Version

Interactive Discussion



Abstract

During KEOPS2 (Kerguelen Ocean and Plateau Compared Study 2), we determined dissolved inorganic and organic nitrogen and phosphorus species in the naturally fertilized region of Kerguelen Island (Southern Ocean). Above 150 m, stations were clearly separated by the Polar Front (PF), with concentrations of NO_3^- , NO_2^- and PO_4^{3-} overall lower north than south of the PF. Though less pronounced, a similar trend was detectable for dissolved organic nitrogen (DON) and phosphorus (DOP). At all stations offshore and above the plateau, a subsurface maximum of NH_4^+ was observed between 50 and 150 m. We examined nutrient stoichiometry by calculating the linear combination $N^* = [\text{NO}_3^-] - 16[\text{PO}_4^{3-}]$. The majority of stations and depths revealed N^* close to $-3 \mu\text{M}$, however, for surface waters north of the PF N^* increased up to $6 \mu\text{M}$. This suggests a preferential uptake of PO_4^{3-} vs. NO_3^- by fast growing diatoms. Using the tracer $\text{TN}_{xs} = [\text{TDN}] - 16[\text{TDP}]$ revealed that the dissolved organic fraction significantly contributed to changes in TN_{xs} . TN_{xs} were negative for most stations and depths, and relatively constant in the layer 0–500 m. As for N^* , the stations north of the PF had higher TN_{xs} in the layer 0–100 m. We discuss this stoichiometric anomaly with respect to possible external sources and sinks of N and P. Additional data collected in February 2013 at two sites revealed the occurrence of a subsurface of N^* located just below the pycnocline that denotes a layer where preferential remineralization of P vs. N persists throughout the season.

1 Introduction

The first scientific expeditions in the Southern Ocean discovered high concentrations of major nutrients such as nitrate (NO_3^-) and phosphate (PO_4^{3-}) in surface waters south of 50°S (Hart, 1942). The general meridional overturning circulation that brings deep water to the surface at the southern limits of the Antarctic circumpolar current (Marshall and Speer, 2012) is the major mechanism supplying surface waters with NO_3^- and

BGD

11, 9949–9977, 2014

Distributions and stoichiometry of dissolved nutrients in the Southern Ocean

S. Blain et al.

[Title Page](#)

[Abstract](#)

[Introduction](#)

[Conclusions](#)

[References](#)

[Tables](#)

[Figures](#)

◀

▶

◀

▶

[Back](#)

[Close](#)

[Full Screen / Esc](#)

[Printer-friendly Version](#)

[Interactive Discussion](#)



PO₄³⁻. Most of the nutrient-rich upwelled waters are transported northward and they leave the surface north of the polar front, through their transformation into intermediate and mode waters. Despite the several months long northward transport during which the NO₃⁻ and PO₄³⁻ rich waters are exposed to sunlight, little phytoplankton biomass develops. This system was characterized as “high nitrate low chlorophyll” (HNLC). The major consequence of the HNLC status of the Southern Ocean is that large amounts of unused nutrients are transported back into the ocean interior where they feed the main thermocline and finally supply low and mid latitude surface waters with essential nutrients (Sarmiento et al., 2004). Another consequence is that similarly to NO₃⁻ and PO₄³⁻, large amounts of upwelled dissolved inorganic carbon (DIC) are not converted to particulate organic carbon (POC) and remain in contact with the atmosphere for time periods long enough to degas carbon dioxide (CO₂) with important consequences on climate (Sigman and Boyle, 2000).

The iron hypothesis (Martin and Fitzwater, 1988) was a major advancement for our understanding of the HNLC paradox. More than two decades of intense research have confirmed that increasing iron supply stimulates primary production, major nutrient utilization and the air-sea flux of CO₂ in surface waters. Nutrient utilization in surface waters is therefore a diagnostic of the efficiency of the biological pump of CO₂. Nitrate utilization has also received much attention in paleoceanographic studies, because it can be inferred from the isotopic composition of N in bulk material or specific compounds of fossil organisms preserved in the sediment. Recent results provide support to the enhanced NO₃⁻ utilization related to higher dust deposition during the ice ages in the sub Antarctic region (Martinez-Garcia et al., 2014).

Many modelling studies on the iron hypothesis, using models that did not explicitly represented the iron cycle, were realized with the extreme assumption that iron fertilization results in the complete depletion of N or P in surface waters (Gnanadesikan et al., 2003). However, this was never observed during artificial iron fertilization (Boyd et al., 2007), iron addition during deck incubations (Moore et al., 2007) or in naturally iron fertilized regions (Blain et al., 2007). For most previous research in this context,

Distributions and stoichiometry of dissolved nutrients in the Southern Ocean

S. Blain et al.

[Title Page](#)

[Abstract](#)

[Introduction](#)

[Conclusions](#)

[References](#)

[Tables](#)

[Figures](#)

◀

▶

◀

▶

[Back](#)

[Close](#)

[Full Screen / Esc](#)

[Printer-friendly Version](#)

[Interactive Discussion](#)



it was assumed that NO_3^- and PO_4^{3-} behave in a similar way. This is only true at first order because interesting differences were noticed. For example, Weber and Deutsch (Weber and Deutsch, 2010) used zonal mean distributions of NO_3^- and PO_4^{3-} in the Southern Ocean to reveal that the differential utilization of both nutrients is likely related to the composition of the phytoplankton community. Detailed investigations of blooms in varying regions of the Southern Ocean confirm different utilization of NO_3^- and PO_4^{3-} depending on the dominant species in the phytoplankton community (Arrigo, 1999; De Baar et al., 1997; Moore et al., 2007).

Our work aims to present a new data set of dissolved nitrogen and phosphorus concentrations, including both inorganic and organic pools. Most of the results are from iron-fertilized regions near the Kerguelen archipelago. Besides the presentation of the distributions and their spatial and temporal variations, we also discuss the stoichiometry of both nutrients.

2 Material and methods

2.1 Sampling

For NO_3^- , PO_4^{3-} and nitrite (NO_2^-), syringes (50 mL) were directly connected to the spigot of the Niskin bottles. The samples were drawn through a 0.45 µm Up-tidisc adapted to the syringe. Duplicate samples were collected. One sample was immediately analyzed aboard. The second sample (25 mL) was poisoned with mercuric chloride (HgCl_2 , 20 mg L⁻¹, final concentration) and stored in the dark at room temperature for later analysis. This second run of analysis in the home laboratory was not done considering the good quality of the analysis performed aboard.

For ammonium (NH_4^+), samples were collected from Niskin bottles in two 50 mL Schott glass bottles. Following rinsing, the bottles were filled with 40 mL of seawater and closed immediately to avoid contamination by air. Back in the aboard laboratory the oxidative reagent (Holmes et al., 1999) was added.

Distributions and stoichiometry of dissolved nutrients in the Southern Ocean

S. Blain et al.

[Title Page](#)

[Abstract](#)

[Introduction](#)

[Conclusions](#)

[References](#)

[Tables](#)

[Figures](#)

◀

▶

◀

▶

[Back](#)

[Close](#)

[Full Screen / Esc](#)

[Printer-friendly Version](#)

[Interactive Discussion](#)



[Title Page](#)[Abstract](#)[Introduction](#)[Conclusions](#)[References](#)[Tables](#)[Figures](#)[◀](#)[▶](#)[◀](#)[▶](#)[Back](#)[Close](#)[Full Screen / Esc](#)[Printer-friendly Version](#)[Interactive Discussion](#)

For dissolved organic nitrogen (DON) and phosphorus (DOP) analysis the samples were collected from Niskin bottles in 100 mL Schott glass bottles. The Schott glass bottles were rinsed with HCl (10 %) and several times with ultrapure water between casts. The samples were then filtered through 2 combusted GF/F filters. 20 mL of the filtered samples were transferred to 20 mL PTFE vials and poisoned with 100 µL of HgCl_2 (4 g L^{-1} , working solution) before storage at 4°C . All analyses were performed aboard as described below.

2.2 Analytical methods

Samples for DON and DOP analysis were spiked with 2.5 mL of the oxidative reagent (boric acid + sodium hydroxide + potassium peroxodisulfate), and then heated at 120°C during 30 min. After cooling, the concentrations of NO_3^- and PO_4^{3-} were determined using continuous flow analysis (Aminot, 2007) with a Skalar instrument.

Samples for NH_4^+ determination were incubated for at least 3 h in the dark, at ambient temperature, before fluorescence measurements ($\lambda_{\text{exc}} = 370 \text{ nm}$ $\lambda_{\text{emi}} = 460 \text{ nm}$) with a fluorimeter (Jabsco).

3 Results

All the stations used in this work are presented in Fig. 1. Most of the stations are located south of the Polar Front (PF), with the exception of the coastal stations TEW-1-2 and the offshore stations TNS-1-2, TEW-7-8 and F-L that were located north of the PF. Station R-2, located west of the plateau had low chlorophyll concentrations in surface water throughout the season, an observation that is explained by the low iron supply (Quéróu et al., 2014). By contrast, all other stations were characterized by the development of large spring blooms consistent with higher iron supply (Lasbleiz et al., 2014). However, the development of the blooms within the iron fertilized region was not homogenous in time and space. A3-1, and stations TNS-1 to TNS-10 of the North-

South transect, sampled at the beginning of the spring bloom, were characterized by low chlorophyll concentrations only slightly higher than that at station R-2. Stations TEW-1 to TEW-8 of the East–West transect, stations E-2 to E-5, and station A3-2 (second visit at station A3), were sampled a few days later, when the bloom rapidly developed with large spatial heterogeneity. The largest stocks of chlorophyll *a* within the 0–200 m layer were observed at stations F-L north of the PF and at station A3-2 above the plateau. Based on the trajectories of 2 surface drifters (Zhou et al., 2014), stations E-1, E-2, E-3, E4-E and E-5, are assumed to evolve in a quasi Lagrangian framework and their succession in time can be considered at the first order as a time series.

3.1 Two dimensional distributions of dissolved nitrogen and phosphorus

In the upper 200 m of the water column, concentrations of NO_3^- and PO_4^{3-} were $\geq 19 \mu\text{M}$ and $\geq 1 \mu\text{M}$, respectively (Figs. 2 and 3). Concentrations were higher west of the PF (transect EW, Fig. 2) and South of the PF (transect NS, Fig. 3) and lower in surface subantarctic waters, north and east of the PF. Concentrations of NO_2^- were the highest above 150 m, and below this depth NO_2^- decreased rapidly to reach values close to the limit of detection at 200 m. Above 150 m, the PF clearly separated the stations located in Antarctic Zone (AZ) (NO_2^- of 0.25 μM) from the stations located in the polar front zone (PFZ) (NO_2^- in the range 0.3–0.4 μM). Along the transect EW, the highest NO_2^- concentrations were measured at TEW-1 (0.31–0.34 μM). Contrasting with the NO_2^- distribution observed along the transect NS, the stations of the AZ (i.e. west of the isocline sigma = 27) had higher concentrations than those of the PFZ. NH_4^+ concentrations were highest at the coastal stations. At Stations TEW-1 and TEW-2, NH_4^+ concentrations increased from 0.19 μM and 0.17 μM (at 10 m), respectively, to 1.45 μM and 0.39 μM (close to the bottom), respectively. At all stations offshore and above the plateau, a subsurface maximum of NH_4^+ peaking at 0.5–0.6 μM was observed between 50 and 150 m. The DON distribution was characterized by a north-south gradient in the

S. Blain et al.

[Title Page](#)[Abstract](#)[Introduction](#)[Conclusions](#)[References](#)[Tables](#)[Figures](#)[◀](#)[▶](#)[◀](#)[▶](#)[Back](#)[Close](#)[Full Screen / Esc](#)[Printer-friendly Version](#)[Interactive Discussion](#)

Title Page

Abstract

Introduction

Conclusions

References

Tables

Figures

◀

▶

◀

▶

Back

Close

Full Screen / Esc

Printer-friendly Version

Interactive Discussion



0–150 m layer. DON concentrations were lowest at Stations A3-1 and TNS-10 (4–7 µM) above the Kerguelen plateau. Intermediate values were found within the PF meander and highest DON concentrations were detectable north of the PF (6–10 µM). For DOP, the latitudinal gradient was less pronounced, but DOP concentrations were lower above the Kerguelen plateau than at any other sites.

3.2 Speciation of dissolved nitrogen at selected sites.

3.2.1 The Kerguelen plateau station A3

The vertical distribution of different chemical nitrogen species during the two visits at station A3 are detailed in Fig. 4. NO_3^- distributions are discussed in more detail in the section “Temporal evolution of vertical distributions of nitrate and phosphate”. Concentrations of NO_2^- were, during both visits, homogeneous in the mixed layer and revealed a small maximum below the mixed layer depth (MLD). NO_2^- increased from 0.27 µM at A3-1 to 0.33 µM at A3-2 (Fig. 4b). NH_4^+ concentrations roughly doubled between the two visits (0.1 µM at A3-1 to 0.2 µM at A3-2) and clear maxima were detectable at the base of the mixed layer. DON accounted for 20 % of TDN in the mixed layer at A3-1, and this contribution increased to 25 % in the upper 40 m water layer at A3-2. This was due to both, NO_3^- consumption and DON release during the 4 weeks that separated the two visits. In the depth layer 40 m to 170 m, however, the contribution of DON was reduced to 17 % indicating a more rapid decrease in DON than in NO_3^- . Below 200 m, the differences in the contributions to TDN are mainly driven by the differences in DON concentrations that were higher at A3-1 (4.7–6.7 µM) than at A3-2 (1.8–4 µM) in the 250–300 m layer (Fig. 4).

3.2.2 Stations F-S and F-L north of the Polar Front

Distinct vertical profiles of NO_2^- and NH_4^+ were observed at station F-S. Concentrations of NO_2^- decreased from 0.39 µM at 10 m to 0.22 µM at 93 m. However, we note a re-

markedly low value of $0.15 \mu\text{M}$ at 79 m (Fig. 5a). The NH_4^+ profile presented the same anomaly, resulting in two subsurface maxima. This feature contrasts with most other stations where a single subsurface maximum was observed, as for example at station F-L (Fig. 5b) located a few nautical miles away from F-S. We suggest that this anomaly is due to the position of F-S within the polar front where a complex mixing event at small scale could have occurred. The contribution of DON to TDN at F-S decreased continuously from 34 % at 20 m to 9 % at 120 m. However, close to the surface the contribution of DON was only 17 % (Fig. 5d).

3.2.3 The HNLC station R-2

- The vertical distribution of NO_3^- and DON revealed small variations between the surface and 200 m (Fig. 6a). DON accounted for 19 % to 24 % of TDN, representing intermediate values as compared to the range observed in the fertilized region. Concentrations of NO_2^- and NH_4^+ presented similar vertical distributions, decreasing rapidly below the mixed layer (Fig. 6b). Concentrations of NH_4^+ in the mixed layer ($0.07 \mu\text{M}$) were at least two fold lower than at any other stations, and NO_2^- concentrations in the mixed layer ($0.3 \mu\text{M}$) were similar to those of the mixed layers in the fertilized regions.

3.2.4 Lagrangian sites E

- All stations were characterized by similar vertical distributions of NO_2^- and NH_4^+ . Concentrations in the mixed layer were in the range $0.25\text{--}0.3 \mu\text{M}$ decreasing to $0.02\text{--}0.03 \mu\text{M}$ below 200 m. The vertical distributions of NH_4^+ are characterized by a subsurface maximum with concentrations ($0.4\text{--}0.65 \mu\text{M}$) two fold higher than at the surface ($0.2\text{--}0.3 \mu\text{M}$). NO_3^- distributions are described in more detail in the next section. The contribution of DON to TDN in the mixed layer was in the range 15–25 %. No clear temporal evolution was detectable.

Distributions and stoichiometry of dissolved nutrients in the Southern Ocean

S. Blain et al.

[Title Page](#)

[Abstract](#)

[Introduction](#)

[Conclusions](#)

[References](#)

[Tables](#)

[Figures](#)

◀

▶

◀

▶

[Back](#)

[Close](#)

[Full Screen / Esc](#)

[Printer-friendly Version](#)

[Interactive Discussion](#)



3.3 Temporal evolution of the vertical distributions of nitrate and phosphate

3.3.1 The Lagrangian sites E

The vertical profiles of NO_3^- and PO_4^{3-} concentrations in the upper 200 m of 5 stations located in the center of a meander of the PF are presented in Fig. 7. In addition, we show data from two other cruises. Samples collected in early October 1995 during the cruise ANTARES3 (Blain et al., 2001) provide data typical of winter conditions. Samples of the KEOPSMOOR profile were collected in February 2013, representing post bloom conditions.

Concentrations of NO_3^- are almost identical among visits at 150 m (mean $27.5 \pm 0.8 \mu\text{mol L}^{-1}$, Fig. 7a). Above 150 m, NO_3^- concentrations change along the season. In winter, concentrations are homogenous from surface to 150 m, resulting in a mean integrated stock of $4.22 \pm 0.08 \text{ mol m}^{-2}$. In spring, the KEOPS2 profiles qualitatively cluster in two groups. The first cluster is composed of stations TNS-5, TNS-6, E-1, E-2 and E-3, with higher NO_3^- concentrations (mean integrated stock 0–150 m of $4.10 \pm 0.05 \text{ mol m}^{-2}$) than in the group formed by stations E4-E and E-5 (mean integrated stock 0–150 m of $3.90 \pm 0.04 \text{ mol m}^{-2}$). Finally, the lowest concentrations were measured in summer (mean integrated stock 0–150 m of 3.48 mol m^{-2}).

Vertical profiles of PO_4^{3-} present similar characteristics as NO_3^- , with the exception of the winter profile (Fig. 7b). The winter profile indicates that PO_4^{3-} concentrations are homogeneously mixed in the upper 150 m. The concentrations seem overestimated at 150 m and above. We do not think that the differences result from inter-annual variability because this would have also impacted NO_3^- concentrations. The high concentrations of PO_4^{3-} measured in winter 1995 lead to a $\text{NO}_3^- : \text{PO}_4^{3-}$ ratio of 12.5 which is low. The overestimation of PO_4^{3-} could results from methodological issues. The ANTARES3 samples were not analyzed aboard, but a few months later in a laboratory by a different analytical protocol. The lack of certified international standards necessary for a strong

BGD

11, 9949–9977, 2014

Distributions and stoichiometry of dissolved nutrients in the Southern Ocean

S. Blain et al.

[Title Page](#)

[Abstract](#)

[Introduction](#)

[Conclusions](#)

[References](#)

[Tables](#)

[Figures](#)

◀

▶

◀

▶

[Back](#)

[Close](#)

[Full Screen / Esc](#)

[Printer-friendly Version](#)

[Interactive Discussion](#)



quality control of the accuracy precludes rigorous comparison of sample collected in 1995 with more recent samples.

Similarly to NO_3^- , we consider the mean concentration of PO_4^{3-} at 150 m (excluding the ANTARES3 PO_4^{3-} value) to estimate a mean winter PO_4^{3-} concentration in the surface layer of $1.93 \pm 0.09 \mu\text{mol L}^{-1}$, that yields an integrated winter stock of $0.30 \pm 0.02 \text{ mol m}^{-2}$. The integrated stock for the group of stations E-1-2-3 ($0.280 \pm 0.004 \text{ mol m}^{-2}$) was higher than for the group E-4-5 ($0.274 \pm 0.005 \text{ mol m}^{-2}$). At the end of the season the integrated PO_4^{3-} stock was 0.250 mol m^{-2} .

3.3.2 The Kerguelen plateau station A3

- 10 A similar seasonal change in NO_3^- and PO_4^{3-} concentrations was observed at Station A3 (Fig. 8). The profiles of both nutrients merge at 200 m in early spring and summer (A3-1 and A3-2). However, during the second visit at A3 (A3-2), we observed that the surface layer was mixed down to 170 m. We propose that the concentrations at 200 m are a good estimate of the winter concentrations of NO_3^- and PO_4^{3-} at this station. Thus,
15 winter stocks ($0\text{--}200 \text{ m}$) were 6.27 and 0.43 mol m^{-2} for NO_3^- and PO_4^{3-} , respectively. At the first visit at station A3 the stocks have decreased to 5.96 and 0.41 mol m^{-2} . Four weeks later (A3-2) they reached 5.29 and 0.36 mol m^{-2} . Finally, in February the stocks were 4.77 and 0.35 mol m^{-2} .

4 Discussion

- 20 The distribution of NO_3^- and PO_4^{3-} in the world's oceans were extensively studied over the past decades. A major rationale for this research is the critical role of these major nutrients for phytoplankton growth and therefore marine primary production. Further, concentrations of NO_3^- and PO_4^{3-} are used as tracers for biogeochemical processes in the ocean (Deutsch and Weber, 2012). In the Southern Ocean, south of the sub-antarctic front, NO_3^- and PO_4^{3-} concentrations are high. They are therefore considered
25

BGD

11, 9949–9977, 2014

Distributions and stoichiometry of dissolved nutrients in the Southern Ocean

S. Blain et al.

[Title Page](#)

[Abstract](#)

[Introduction](#)

[Conclusions](#)

[References](#)

[Tables](#)

[Figures](#)



[Back](#)

[Close](#)

[Full Screen / Esc](#)

[Printer-friendly Version](#)

[Interactive Discussion](#)



Distributions and stoichiometry of dissolved nutrients in the Southern Ocean

S. Blain et al.

[Title Page](#)

[Abstract](#)

[Introduction](#)

[Conclusions](#)

[References](#)

[Tables](#)

[Figures](#)

◀

▶

◀

▶

[Back](#)

[Close](#)

[Full Screen / Esc](#)

[Printer-friendly Version](#)

[Interactive Discussion](#)



as non-limiting and much less attention has been paid to their distribution if compared to other nutrients such as silicic acid or dissolved iron. However, the relief of iron limitation by natural or artificial fertilizations offers a different perspective because NO_3^- and PO_4^{3-} should be consumed as the bloom develops. This has motivated the present detailed study of dissolved N and P in the naturally fertilized region of Kerguelen.

To explore the dynamics of NO_3^- and PO_4^{3-} we examined their stoichiometry in the study region. This is commonly done by establishing the ratio $r_{\text{N:P}} = [\text{NO}_3^-] : [\text{PO}_4^{3-}]$ for comparison with the Redfield ratio of 16. However, the use of $r_{\text{N:P}}$ is limited because this ratio is not conserved by mixing or biological processes such as uptake or remineralisation (Deutsch and Weber, 2012). We therefore calculated the linear combination $N^* = [\text{NO}_3^-] - 16[\text{PO}_4^{3-}]$, similar to the parameter first introduced by (Michaels et al., 1996), but omitting the constant term required to obtain a global average of N^* equal to 0. N^* traces the impact of processes that add or remove N and P with a stoichiometry different from the Redfield ratio of 16. At almost all stations and depths, N^* was close to $-3 \mu\text{M}$ (Fig. 9a). This value agrees well with the mean N^* computed for regions of the Southern Ocean close to the PF (Weber and Deutsch, 2010). A noticeable deviation from this value was observed for a set of data where N^* increased from $N^* = -3 \mu\text{M}$ to $N^* = 6 \mu\text{M}$. All data with $N^* > 0$ are for samples collected in the mixed layer north of the PF, and located in a large diatom bloom (Lasbleiz et al., 2014).

Nutrient drawdown lower than the Redfield ratio was observed previously in the Southern Ocean. During the artificial iron fertilization experiment EIFEX, an apparent differential consumption of $\Delta(\text{NO}_3^-) : \Delta(\text{PO}_4^{3-})$ of 6.4 was reported (Smetacek et al., 2012). Arrigo et al. (1999) and De Baar et al. (1997) determined a nutrient drawdown ratio in diatom blooms of 9.7 and 4.4–6.1, respectively. Near Crozet, the removal of NO_3^- vs. PO_4^{3-} measured in situ and during iron addition experiments revealed that the ratio was inversely related to the proportion of diatoms of the phytoplankton community (Moore et al., 2007). All these studies confirm the impact of diatom blooms on nutrient stoichiometry in the surface layer. However, the interpretations of these observations are diverse. De Baar et al. (1997) suggested that the preferential drawdown of PO_4^{3-}

during the bloom of *Fragilaropsis kerguelensis* in the PF could be due to the reduction of nitrate reductase activity by iron limitation or due to the dominance of *Fragilaropsis kerguelensis* with low N:P ratios considered as a specific physiological trait. These hypotheses could not explain our observations because the stations with a nutrient drawdown anomaly were located in an iron fertilized region and the diatom community was not dominated by *Fragilaropsis kerguelensis* (M. Lasbleiz, personal communication, 2014).

Thus, we interpret the positive values of N^* as a result of the preferential uptake of PO_4^{3-} vs. NO_3^- by fast growing diatoms. Diatoms have a mean elemental N:P stoichiometry of 10 ± 4 (Sarthou et al., 2005) that differs from the Redfield value. Indeed, the elemental particulate matter composition determined at the stations with positive N^* during KEOPS2 (Lasbleiz et al., 2014) exhibits a mean ratio of PON:POP of 10.5 ± 3.3 which is consistent with the observed nutrient drawdown $\Delta(\text{NO}_3^-) : \Delta(\text{PO}_4^{3-})$ of 8. We suggest that the preferential allocation of resources to the P-rich assembly of the cell machinery by exponentially growing cells is the most likely explanation for our observations (Klausmeier et al., 2004). The anomaly observed for the present data set is not linked to a particular species but to general traits of the diatom community responding to iron fertilization.

As a variant of N^* , the tracer DIN_{xs} , takes into account NO_3^- and NH_4^+ (Hansell et al., 2007), but none of those tracers consider the organic pools of N and P. Landolfi et al. (2008) have defined the tracer $\text{TN}_{xs} = [\text{TDN}] - 16[\text{TDP}]$ and have shown that the dissolved organic fraction significantly contributes to changes in TN_{xs} . For example, relying on N^* only, can lead to an underestimation of N_2 fixation at the global scale (Landolfi et al., 2008). We have therefore calculated TDN and TDP at all KEOPS2 stations where DON and DOP measurements were available (Fig. 9b). $\text{TDN} = f(\text{TDP})$ reveals more dispersion of the data than $\text{NO}_3^- = f(\text{PO}_4^{3-})$, mainly due to the lower analytical precision for DOP and DON determinations. Still, clear trends are detectable. TN_{xs} were negative for most stations and depths, and relatively constant in the layer 0–500 m. As for N^* the stations north of the PF had higher TN_{xs} in the layer 0–100 m.

Distributions and stoichiometry of dissolved nutrients in the Southern Ocean

S. Blain et al.

[Title Page](#)

[Abstract](#)

[Introduction](#)

[Conclusions](#)

[References](#)

[Tables](#)

[Figures](#)

◀

▶

◀

▶

[Back](#)

[Close](#)

[Full Screen / Esc](#)

[Printer-friendly Version](#)

[Interactive Discussion](#)



Distributions and stoichiometry of dissolved nutrients in the Southern Ocean

S. Blain et al.

When a water parcel is considered, N^* is affected by the redistribution of N and P between the inorganic and the organic pools, whereas TN_{xs} is only affected by net non-redfieldien sources or sinks of N and P. Consequently, the positive anomaly observed for TN_{xs} in surface waters north of the PF can be explained by three possible mechanisms: deposition of N rich material from the atmosphere, N_2 fixation and export of P rich material. The region of Kerguelen receives low quantities of atmospheric material (Heimbürger et al., 2012; Wagener et al., 2008) which is mainly from natural origin, such as desert dust, that contains little nitrogen compared to phosphorus (Zamora et al., 2013). This is confirmed by the low N deposition rate estimated around Crozet Island ($2 \text{ nmol m}^{-2} \text{ d}^{-1}$; Planquette et al., 2007). We can therefore refute the deposition of N rich material as the cause of the TN_{xs} anomaly. The second hypothesis involves N_2 fixation. To date, N_2 fixation was not reported to occur in the cold waters of the Southern Ocean. However, during KEOPS2 detectable N_2 fixation rates were measured at different stations with a few exceptionally high values ($\sim 250 \mu\text{mol m}^{-2} \text{ d}^{-1}$) in the mixed layer of station F-L (C. Fernandez, personal communication, 2014). Such high fixation rates could contribute to an enrichment of about 1 % of TDN that is not enough to create the observed anomaly. If N_2 fixation was a dominant process driving the N:P stoichiometry at this station, POM elemental composition should be also affected. Generally, N_2 fixing microorganisms have a high N:P ratio (Laroche and Breitbarth, 2005). Such high ratios are at odds with the low N:P measured in the POM at station F-L (Lasbleiz et al., 2014). The third hypothesis for explaining the anomaly relies on the export of P rich material from the mixed layer. We do not have direct measurements of N:P in the exported material, but we already mentioned above that the elemental composition of particulate matter at station F-L yielded the lowest N:P ratio in POM (Lasbleiz et al., 2014). This provides support that the export of P rich material could result in high TN_{xs} values north of the PF. We propose that the anomaly of TN_{xs} results from the imprint on stoichiometry of the diatom bloom which consumed and exported phosphorus in a ratio below the Redfield value.

[Title Page](#)[Abstract](#)[Introduction](#)[Conclusions](#)[References](#)[Tables](#)[Figures](#)[◀](#)[▶](#)[◀](#)[▶](#)[Back](#)[Close](#)[Full Screen / Esc](#)[Printer-friendly Version](#)[Interactive Discussion](#)

Distributions and stoichiometry of dissolved nutrients in the Southern Ocean

S. Blain et al.

[Title Page](#)[Abstract](#)[Introduction](#)[Conclusions](#)[References](#)[Tables](#)[Figures](#)[◀](#)[▶](#)[◀](#)[▶](#)[Back](#)[Close](#)[Full Screen / Esc](#)[Printer-friendly Version](#)[Interactive Discussion](#)

During KEOPS2 rapidly growing diatom blooms were also sampled at other stations located south of the PF, but anomalies similar to those at F-L were not observed. We discussed here the case of stations A3 and E-4W, which had similar chlorophyll concentrations as F-L. There is no reason that the physiological features of exponentially growing diatoms mentioned at F-L do not apply to the diatoms growing at stations A3 and E4-W. It is, however, possible that this effect is not large enough to translate into N^* or TN_{xs} anomalies. A possible explanation could be the differences in the age of the blooms. A younger bloom would have less affected the stoichiometry as compared to a bloom of longer duration. This hypothesis cannot be fully verified due to the poor temporal resolution of the satellite ocean color images available. Another or complementary explanation is the difference in mixed layer depths that were 50 m and 150 m at stations F-L and A3-2, respectively. Such a deep mixed layer as observed at station A3-2 resulted likely from a deep episodic mixing event generated by strong wind prevailing during the day preceding our visit. The deepening could have dampened the anomaly by diluting and mixing the affected water parcel with underlying water having a typical stoichiometry (e.g. N^* or TN_{xs} around -3).

In February 2013, two years after the KEOPS2 cruise, we had the possibility to return to two sites visited during KEOPS2 (stations A3 and TNS-6), and obtain measurements for the concentrations of NO_3^- and PO_4^{3-} . These data, in combination with KEOPS2 data allowed us to compare N^* during two different seasons (Fig. 10). In the mixed layer, little changes of N^* were observed between spring and summer. However, in summer, N^* exhibited a clear subsurface minimum between 100–200 m, at both stations. Denitrification is a process that could produce this subsurface feature. But denitrification would require low oxygen concentrations that are not observed at these stations. We propose that highly negative values of N^* result from preferential remineralisation of P vs. N. In a general manner, preferential remineralisation of P vs. N in the water column is supported by an increase of N:P in high molecular dissolved organic matter (Clark et al., 1998) in particulate matter (Copin-Montegut and Copin-Montegut, 1978) and in supernatant of sediment trap material (Loureys et al., 2003). The observation

of the N^* subsurface minimum at the end of the season, but not at the beginning implies a temporal cumulative effect. The minimum is located just below the mixed layer in the region of the pycnocline that presents the highest density gradient. This could represent a zone with a higher residence time for sinking particles resulting in an accumulation of biomass. Consequently, the remineralization would also be increased in this layer compared to the rest of the water column resulting in a higher accumulation of PO_4^{3-} relative to NO_3^- . The subsurface minimum being located above 200 m depth, it is erased when the winter mixing occurs.

To our knowledge such a subsurface minimum has not been reported in the Southern Ocean. This could be due to the limited studies that investigate concurrently dissolved N and P biogeochemistry, and due to the lack of samples collected at the appropriate vertical and temporal time scale. Our finding raises several further questions. Is the subsurface minimum of N^* a particular feature of iron fertilized regions? What is the link between its occurrence and the strength of stratification of the water column? And what is the role of this layer in the remineralisation of carbon? These questions argue for future detailed investigations of the cycling of both elements in the upper layer of the Southern Ocean.

Acknowledgements. We thank the chief scientist Bernard Quéguiner, the captain Bernard Lassiette and crew of the R/V *Marion Dufresne* for their support aboard. We thank C. Lo Monaco for providing us with the CTD profiles of KEOPSMOOR. This work was supported by the French Research program of INSU-CNRS LEFE-CYBER (Les enveloppes fluides et l'environnement –Cycles biogéochimiques, environnement et ressources), the French ANR (Agence Nationale de la Recherche, SIMI-6 program, ANR-10-BLAN-0614), the French CNES (Centre National d'Etudes Spatiales) and the French Polar Institute IPEV (Institut Polaire Paul-Emile Victor).

Distributions and stoichiometry of dissolved nutrients in the Southern Ocean

S. Blain et al.

[Title Page](#)

[Abstract](#)

[Introduction](#)

[Conclusions](#)

[References](#)

[Tables](#)

[Figures](#)



[Back](#)

[Close](#)

[Full Screen / Esc](#)

[Printer-friendly Version](#)

[Interactive Discussion](#)



References

Distributions and stoichiometry of dissolved nutrients in the Southern Ocean

S. Blain et al.

Title Page

Abstract

Introduction

Conclusions

References

Tables

Figures

◀

▶

◀

▶

Back

Close

Full Screen / Esc

Printer-friendly Version

Interactive Discussion



Distributions and stoichiometry of dissolved nutrients in the Southern Ocean

S. Blain et al.

[Title Page](#)

[Abstract](#)

[Introduction](#)

[Conclusions](#)

[References](#)

[Tables](#)

[Figures](#)

◀

▶

◀

▶

[Back](#)

[Close](#)

[Full Screen / Esc](#)

[Printer-friendly Version](#)

[Interactive Discussion](#)



- Gnanadesikan, A., Sarmiento, J. L., and Slater, R. D.: Effects of patchy ocean fertilization on atmospheric carbon dioxide and biological production, *Global Biogeochem. Cy.*, 17, doi:10.1029/2002GB001940, 2003.
- Hansell, D. A., Olson, D. B., Dentener, F., and Zamora, L. M.: Assessment of excess nitrate development in the subtropical North Atlantic, *Mar. Chem.*, 206, 562–579, 2007.
- Hart, T. J.: Phytoplankton periodicity in Antarctic surface water, *Discov. Rep.*, VIII, 1–268, 1942.
- Heimbürger, A., Losno, R., Triquet, S., Dulac, F., and Mahowald, N.: Direct measurements of atmospheric iron, cobalt, and aluminum-derived dust deposition at Kerguelen Islands, *Global Biogeochem. Cy.*, 26, GB4016, doi:10.1029/2012GB004301, 2012.
- Holmes, R. M., Aminot, A., Kérouel, R., Hooker, B., and Peterson, B.: a simple and precise method for measuring ammonium in marine and freshwater ecosystem, *Mar. Chem.*, 56, 1801–1808, 1999.
- Klausmeier, C. A., Litchman, E., Daufresne, T., and Levin, S. A.: Optimal nitrogen-to-phosphorus stoichiometry of phytoplankton, *Nature*, 429, 171–174, doi:10.1038/nature02454, 2004.
- Landolfi, A., Oschlies, A., and Sanders, R.: Organic nutrients and excess nitrogen in the North Atlantic subtropical gyre, *Biogeosciences*, 5, 1199–1213, doi:10.5194/bg-5-1199-2008, 2008.
- Laroche, J. and Breitbarth, E.: Importance of the diazotrophs as a source of new nitrogen in the ocean, *J. Sea Res.*, 53, 67–91, 2005.
- Lasbleiz, M., Leblanc, K., Blain, S., Ras, J., Cornet-Barthaux, V., Hélias Nunige, S., and Quéguiner, B.: Pigments, elemental composition (C, N, P, Si) and stoichiometry of particulate matter, in the naturally iron fertilized region of Kerguelen in the Southern Ocean, *Biogeosciences Discuss.*, 11, 8259–8324, doi:10.5194/bgd-11-8259-2014, 2014.
- Loureys, M. J., Trull, T. W., and Sigman, D. M.: Sensitivity of $\delta^{15}\text{N}$ of nitrate, surface suspended and deep sinking particulate nitrogen to seasonal nitrate depletion in the Southern Ocean, *Global Biogeochem. Cy.*, 17, 1081, doi:10.1029/2002GB001973, 2003.
- Marshall, J. and Speer, K.: Closure of the meridional overturning circulation through Southern Ocean upwelling, *Nat. Geosci.*, 5, 171–180, doi:10.1038/ngeo1391, 2012.
- Martin, J. M. and Fitzwater, S. E.: Iron deficiency limits phytoplankton growth in the north-east Pacific subarctic, *Nature*, 331, 341–343, 1988.

- Martinez-Garcia, A., Sigman, D. M., Ren, H., Anderson, R. F., Straub, M., Hodell, D. A., Jaccard, S. L., Eglinton, T. I., and Haug, G. H.: Iron fertilization of the Subantarctic Ocean during the last ice age, *Science*, 343, 1347–1350, doi:10.1126/science.1246848, 2014.
- Michaels, A. F., Olson, D., Sarmiento, J., Ammerman, J. W., Fanning, K. A., Jahnke, R. A.,
5 Knap, A. H., Lipschultz, F., and Prospero, J. M.: Inputs, losses and transformations of nitrogen and phosphorus in the pelagic North Atlantic Ocean, *Biogeochemistry*, 35, 181–226, 1996.
- Moore, C. M., Hickman, A. E., Poulton, A. J., Seeyave, S., and Lucas, M. I.: Iron-light interactions during the CROZet natural iron bloom and EXport experiment (CROZEX): II –
10 Taxonomic responses and elemental stoichiometry, *Deep-Sea Res. Pt. II*, 54, 2066–2084, doi:10.1016/j.dsr2.2007.06.015, 2007.
- Planquette, H., Statham, P. J., Fones, G., Charette, M. A., Moore, C. M., Salter, I., Nédélec, F. H., Taylor, S. L., French, M., Baker, A. R., Mahowald, N., and Jickells, T. D.: Dissolved iron in the vicinity of the Crozet islands, Southern Ocean, *Deep-Sea Res. Pt. II*, 54, 1999–2019, 2007.
- Sarmiento, J. L., Gruber, N., Brzezinsky, M. A., and Dunne, J. P.: High-latitude controls of thermocline nutrients and low latitude biological productivity, *Nature*, 427, 56–60, 2004.
- Sarthou, G., Timmermans, K. R., Blain, S., and Treguer, P.: Growth physiology and fate of diatoms in the ocean: a review, *J. Sea Res.*, 53, 25–42, 2005.
- Sigman, D. M. and Boyle, E. A.: Glacial/interglacial variations in atmospheric carbon dioxide,
20 *Science*, 407, 859–869, 2000.
- Smetacek, V., Klaas, C., Strass, V. H., Assmy, P., Montresor, M., Cisewski, B., Savoye, N., Webb, A., d' Ovidio, F., Arrieta, J. M., Bathmann, U., Bellerby, R., Berg, G. M., Croot, P., Gonzalez, S., Henjes, J., Herndl, G. J., Hoffmann, L. J., Leach, H., Losch, M., Mills, M. M., Neill, C., Peeken, I., Röttgers, R., Sachs, O., Sauter, E., Schmidt, M. M., Schwarz, J., Terbrüggen, A., and Wolf-Gladrow, D.: Deep carbon export from a Southern Ocean iron-fertilized
25 diatom bloom, *Nature*, 487, 313–319, doi:10.1038/nature11229, 2012.
- Wagener, T., Guieu, C., Losno, R., Bonnet, S., and Mahowald, N.: Revisiting atmospheric dust export to the Southern Hemisphere ocean: biogeochemical implication, *Global Biogeochem. Cy.*, 22, GB2006, doi:10.1029/2007GB002984, 2008.
- Weber, T. S. and Deutsch, C.: Ocean nutrient ratios governed by plankton biogeography, *Nature*, 467, 550–554, doi:10.1038/nature09403, 2010.

Distributions and stoichiometry of dissolved nutrients in the Southern Ocean

S. Blain et al.

[Title Page](#)

[Abstract](#)

[Introduction](#)

[Conclusions](#)

[References](#)

[Tables](#)

[Figures](#)

◀

▶

◀

▶

[Back](#)

[Close](#)

[Full Screen / Esc](#)

[Printer-friendly Version](#)

[Interactive Discussion](#)



Zamora, L. M., Prospero, J. M., Hansell, D. A., and Trapp, J. M.: Atmospheric P deposition to the subtropical North Atlantic: sources, properties, and relationship to N deposition, *J. Geophys. Res.-Atmos.*, 118, 1546–1562, doi:10.1002/jgrd.50187, 2013.

5 Zhou, M., Zhu, Y., d'Ovidio, F., Park, Y.-H., Durand, I., Kestenare, E., Sanial, V., Van-Beek, P., Queguiner, B., Carlotti, F., and Blain, S.: Surface currents and upwelling in Kerguelen Plateau regions, *Biogeosciences Discuss.*, 11, 6845–6876, doi:10.5194/bgd-11-6845-2014, 2014.

Distributions and stoichiometry of dissolved nutrients in the Southern Ocean

S. Blain et al.

[Title Page](#)

[Abstract](#)

[Introduction](#)

[Conclusions](#)

[References](#)

[Tables](#)

[Figures](#)

◀

▶

[Back](#)

[Close](#)

[Full Screen / Esc](#)

[Printer-friendly Version](#)

[Interactive Discussion](#)



Distributions and stoichiometry of dissolved nutrients in the Southern Ocean

S. Blain et al.

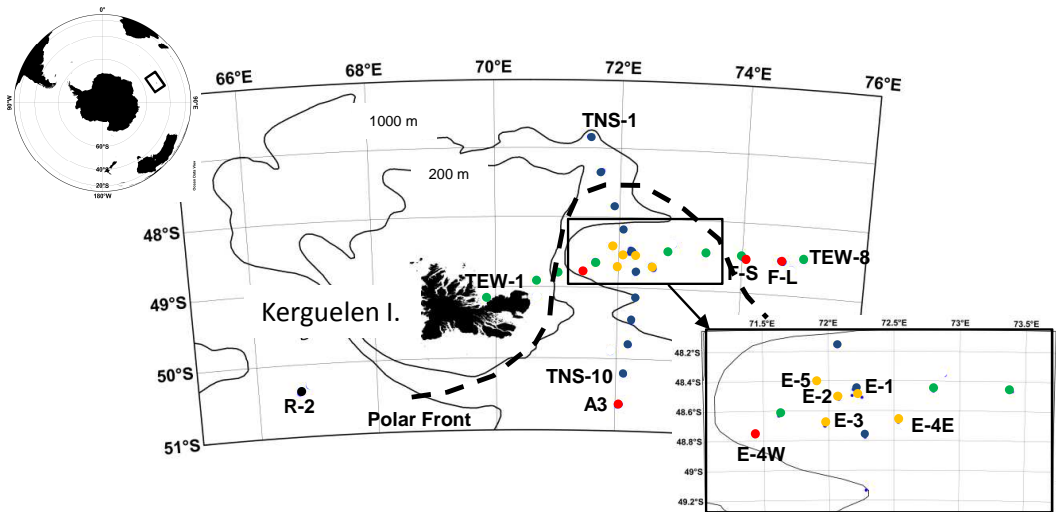


Figure 1. Map of the KEOPS2 study area. The locations of the stations are marked by color dots. Blue indicates the stations of the North–South transect (TNS), green indicates the stations of the East–West transect (TEW), orange indicates the stations E located in the meander of the polar front (zoom panel). Red stands for other stations located in the fertilized region and black stands for the station located in the HNLC region.

[Title Page](#)

[Abstract](#)

[Introduction](#)

[Conclusions](#)

[References](#)

[Tables](#)

[Figures](#)

[◀](#)

[▶](#)

[◀](#)

[▶](#)

[Back](#)

[Close](#)

[Full Screen / Esc](#)

[Printer-friendly Version](#)

[Interactive Discussion](#)

Distributions and stoichiometry of dissolved nutrients in the Southern Ocean

S. Blain et al.

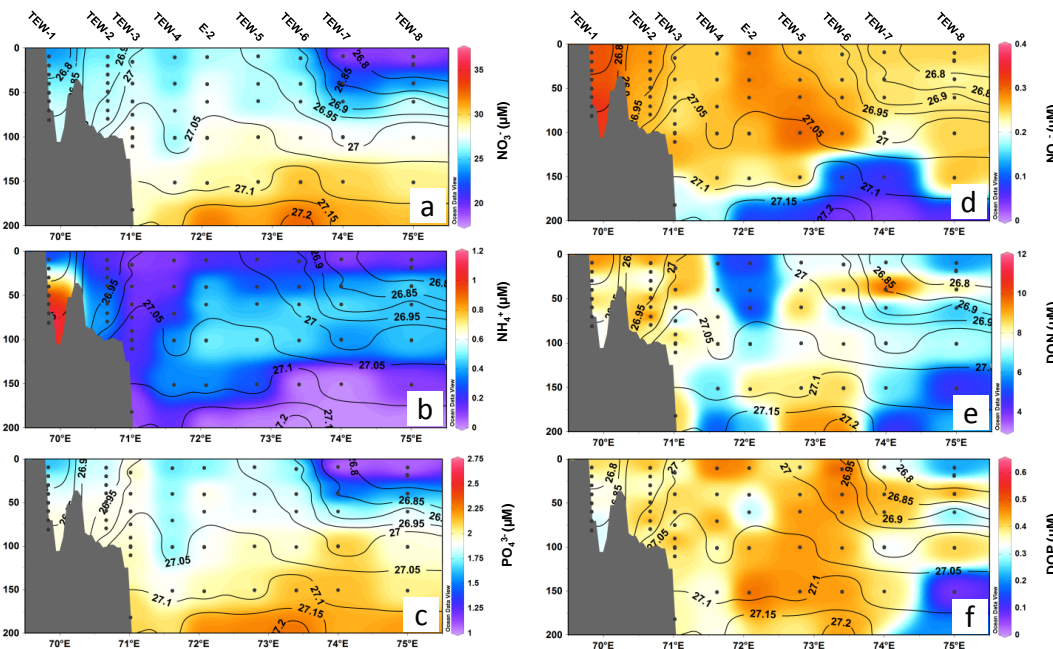


Figure 2. Two dimensional distribution of dissolved nitrogen and phosphorus species along the East–West transect (TEW). **(a)** Nitrate, **(b)** ammonium, **(c)** phosphate, **(d)**, nitrite, **(e)** dissolved organic nitrogen, **(f)** dissolved organic phosphorus. The isolines for sigma are plotted on each panel.

[Title Page](#)

[Abstract](#)

[Introduction](#)

[Conclusions](#)

[References](#)

[Tables](#)

[Figures](#)

[◀](#)

[▶](#)

[◀](#)

[▶](#)

[Back](#)

[Close](#)

[Full Screen / Esc](#)

[Printer-friendly Version](#)

[Interactive Discussion](#)

Distributions and stoichiometry of dissolved nutrients in the Southern Ocean

S. Blain et al.

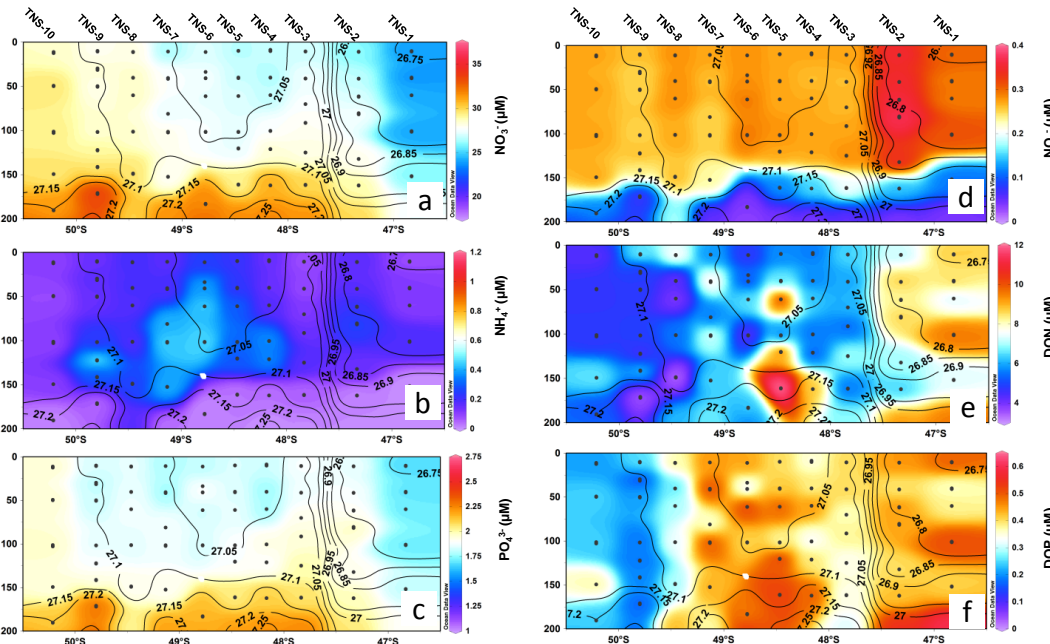


Figure 3. Two dimensional distribution of dissolved nitrogen and phosphorus species along the North–South transect (TNS). **(a)** Nitrate, **(b)** ammonium, **(c)** phosphate, **(d)**, nitrite, **(e)** dissolved organic nitrogen, **(f)** dissolved organic phosphorus. The isolines for sigma are plotted on each panel.

Distributions and stoichiometry of dissolved nutrients in the Southern Ocean

S. Blain et al.

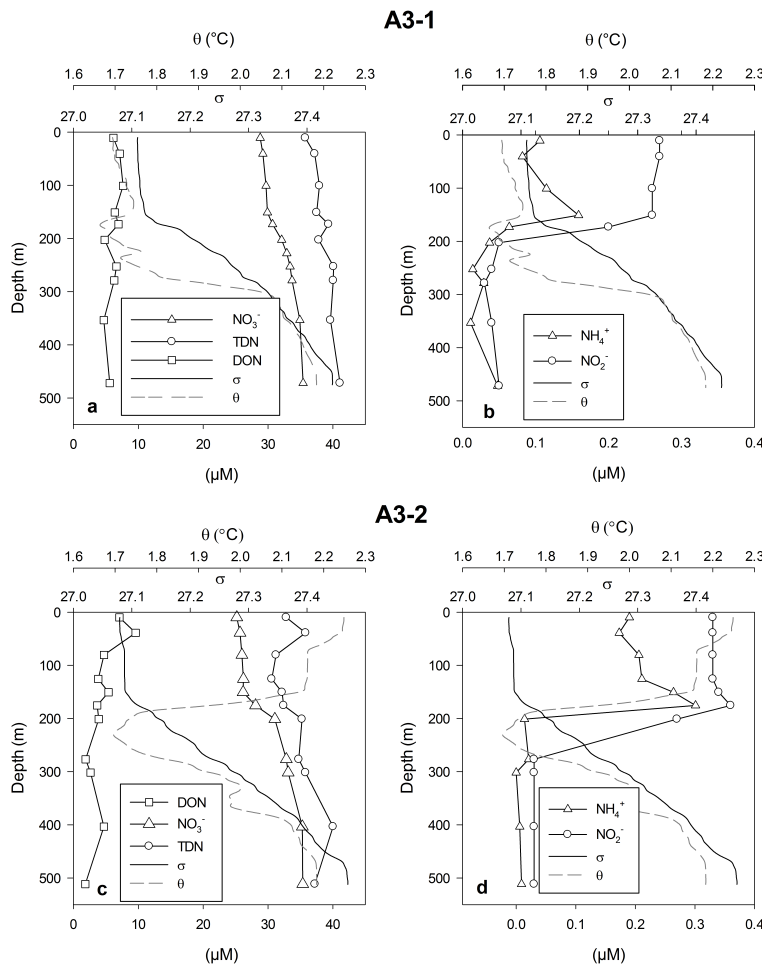


Figure 4. Dissolved nitrogen speciation at station A3-1 (**a, b**) and at station A3-2 (**c, d**) during KEOPS2. Depth profiles of temperature and sigma are plotted on each panel.

[Title Page](#)

[Abstract](#)

[Introduction](#)

[Conclusions](#)

[References](#)

[Tables](#)

[Figures](#)

◀

▶

◀

▶

[Back](#)

[Close](#)

[Full Screen / Esc](#)

[Printer-friendly Version](#)

[Interactive Discussion](#)

Distributions and stoichiometry of dissolved nutrients in the Southern Ocean

S. Blain et al.

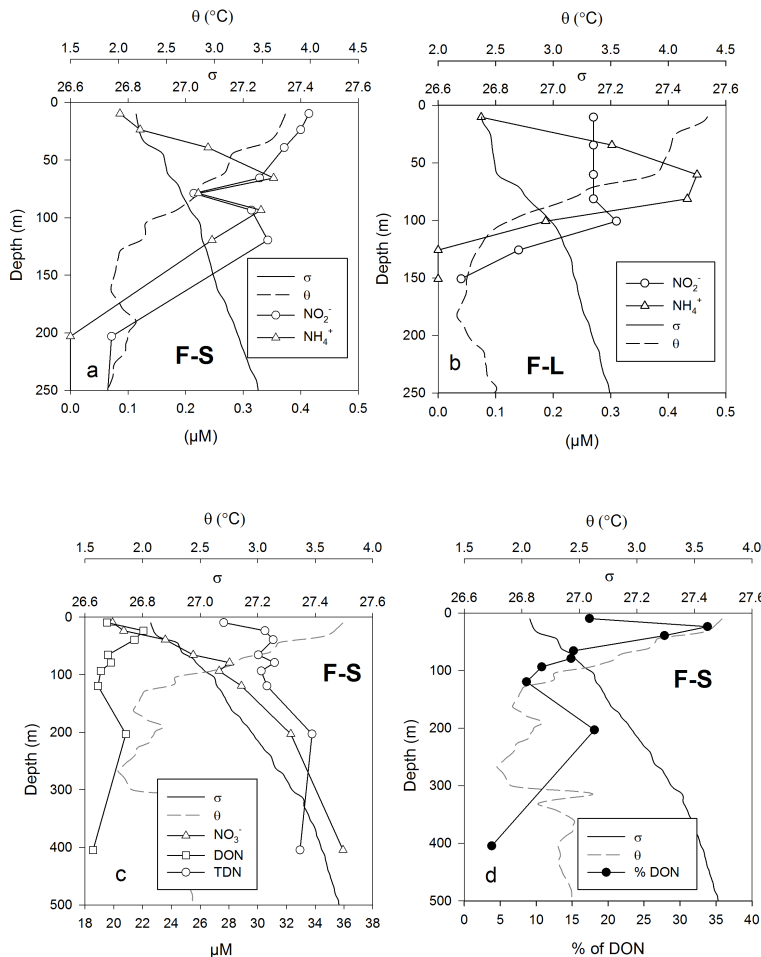


Figure 5. Dissolved nitrogen speciation at stations F-L and F-S during KEOPS2.

[Title Page](#)

[Abstract](#)

[Introduction](#)

[Conclusions](#)

[References](#)

[Tables](#)

[Figures](#)

[◀](#)

[▶](#)

[◀](#)

[▶](#)

[Back](#)

[Close](#)

[Full Screen / Esc](#)

[Printer-friendly Version](#)

[Interactive Discussion](#)

Distributions and stoichiometry of dissolved nutrients in the Southern Ocean

S. Blain et al.

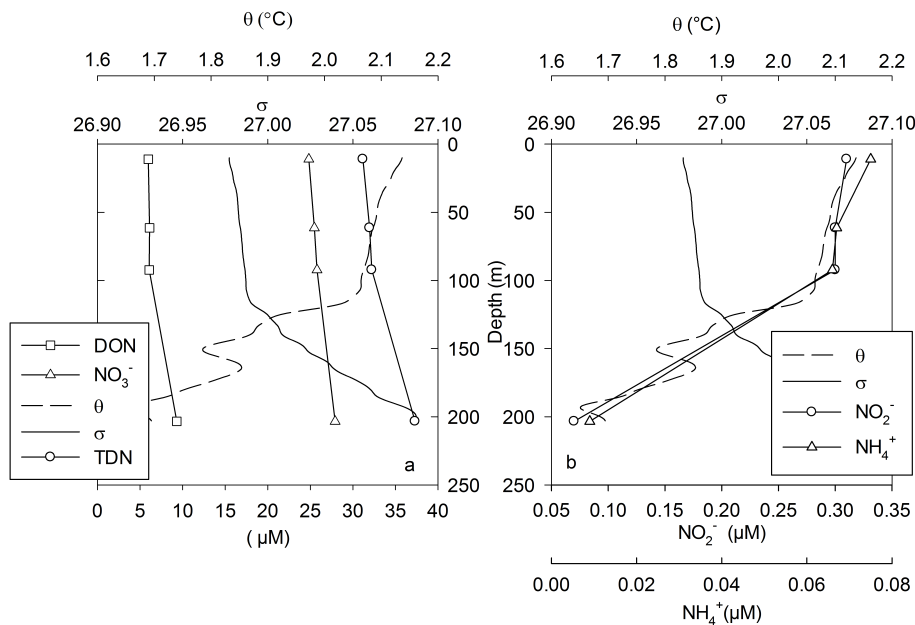


Figure 6. Dissolved nitrogen speciation at station R-2.

Distributions and stoichiometry of dissolved nutrients in the Southern Ocean

S. Blain et al.

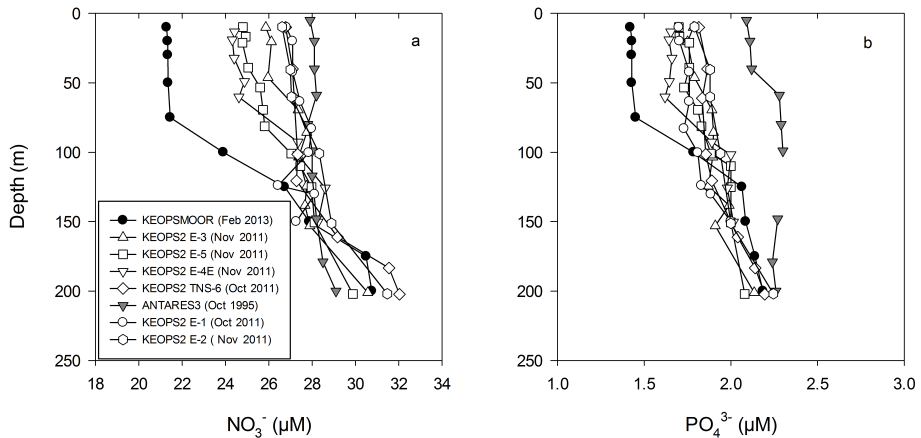


Figure 7. Temporal variability of the vertical profiles of concentrations of NO_3^- (a) and PO_4^{3-} (b) for stations located in the meander of the Polar Front. Details for profiles of KEOPSMOOR (February 2013) and ANTARES3 (October 1995) are provided in the text.

Distributions and stoichiometry of dissolved nutrients in the Southern Ocean

S. Blain et al.

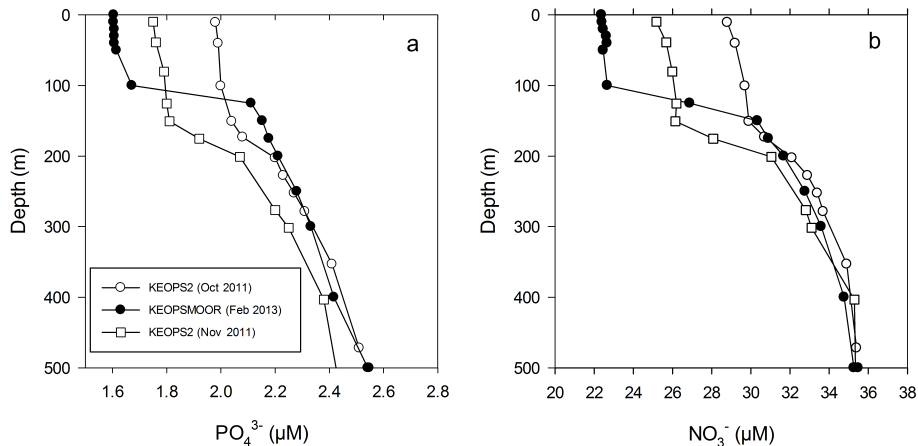


Figure 8. Temporal variability of the vertical profiles of concentrations of PO_4^{3-} (a) and NO_3^- (b) at the station A3.

- [Title Page](#)
- [Abstract](#) [Introduction](#)
- [Conclusions](#) [References](#)
- [Tables](#) [Figures](#)
- [◀](#) [▶](#)
- [◀](#) [▶](#)
- [Back](#) [Close](#)
- [Full Screen / Esc](#)
- [Printer-friendly Version](#)
- [Interactive Discussion](#)

Distributions and stoichiometry of dissolved nutrients in the Southern Ocean

S. Blain et al.

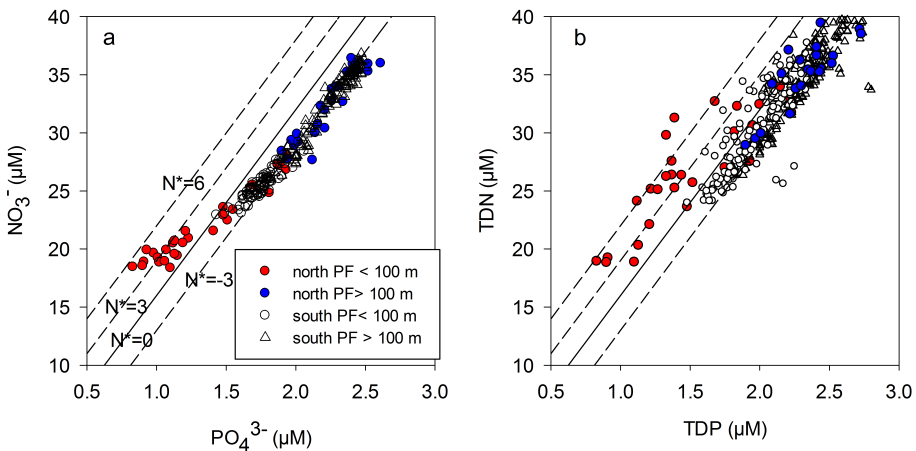


Figure 9. (a) Comparison of concentrations of NO_3^- vs. PO_4^{3-} (dots) with $N^* = \text{NO}_3^- - r_{\text{N:P}}\text{PO}_4^{3-}$ (lines) calculated for different values of $r_{\text{N:P}}$. (b) Comparison of concentrations of TDN vs. TDP with $\text{TN}_{\text{xs}} = \text{TDN} - r_{\text{N:P}}\text{TDP}$ (lines) calculated for different values of $r_{\text{N:P}}$. For both panels the black line correspond to $r_{\text{N:P}} = 16$ (N^* or $\text{TN}_{\text{xs}} = 0$).

Title Page

Abstract

Introduction

Conclusio

References

Tables

Figures



Distributions and stoichiometry of dissolved nutrients in the Southern Ocean

S. Blain et al.

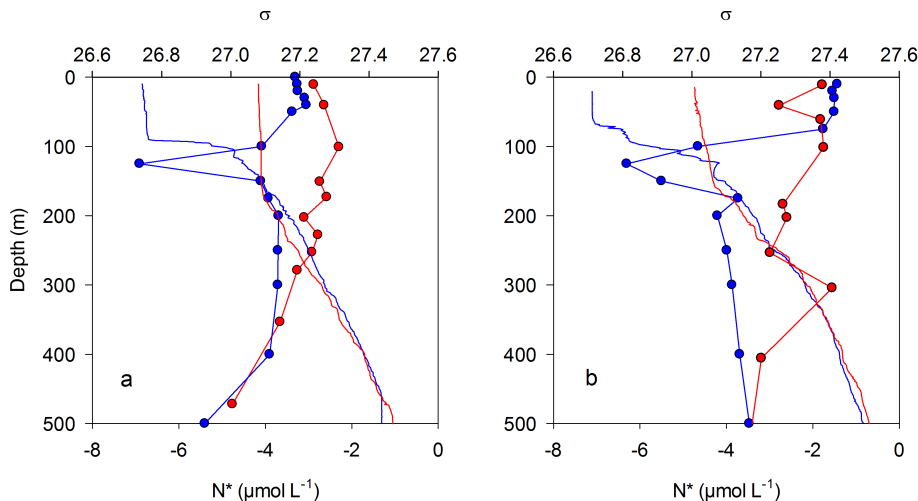


Figure 10. Depth profiles of N^* at stations A3 (a) and TNS-6 (b) for the month of November (in red) and February (in blue). Vertical profiles of sigma are shown with the same color code.